



# Supplementary Materials for

## Imaging of a Circumsolar Dust Ring near the Orbit of Venus

M. H. Jones,\* D. Bewsher, D. S. Brown

\*Corresponding author. E-mail: [m.h.jones@open.ac.uk](mailto:m.h.jones@open.ac.uk)

Published 22 November 2013, *Science* **342**, 960 (2013)  
DOI: 10.1126/science.1243194

**This PDF file includes:**

Materials and Methods  
Supplementary Text  
Figs. S1 and S2  
Table S1  
References

## Materials and Methods

The model of the dust ring is assumed to be co-planar with the orbit of Venus because of the good correspondence between the location of the maximum surface brightness in the maps and the tangent to the orbit of Venus (Fig. 3A). Hence the ring has the same inclination ( $3.39^\circ$ ) and longitude of ascending node ( $76.68^\circ$ ) as Venus. In calculating the scattered light from dust in this ring, a Henyey-Greenstein phase function appropriate for optical scattering (23) was adopted.

Initial parameter fitting was carried out with  $\sigma_z$  as a free parameter (in addition to  $n_{0,\theta}$ ,  $n_{1,\theta}$ ,  $r_0$ , and  $r_1$ ). This however resulted in considerable variation in all the fitted values. Consequently, the weighted mean value of  $\sigma_z = 0.055 \pm 0.003$  AU from all four (HI-2A) data sets was adopted, and the fitting repeated with  $\sigma_z$  fixed as described in the main text.

The fitting of the parameters of the three-dimensional dust model to the maps of HI-2A surface brightness was carried out by  $\chi^2$  minimization (using the Levenberg-Marquardt method). For each iteration of the model fitting process, a synthetic image was generated as follows. A grid was defined which is identical to the coarse grid used for the initial analysis of Level-1 data (i.e. helioecliptic longitude in cells of  $0.5^\circ$  resolution with cell centers from  $35.25^\circ$  to  $59.75^\circ$ , and ecliptic latitude in cells of  $1.0^\circ$  resolution with cell centers from  $-8.0^\circ$  to  $+8.0^\circ$ ). To model a particular data set, a model surface brightness map was generated to correspond to every fifth input Level-1 data file in the set. This was found to be sufficient to account for the changes in viewing geometry during a 10-day integration. Thus the simulation of a 10-day integration period involved 24 model maps (in comparison to 120 data maps). The model maps were averaged before the scan at each value of  $\beta$  was subject to box-car filtering (with a filter width of 13 cells, i.e.  $6.5^\circ$ ) as used in the analysis of the data. Note that the fitting of a power-law and the subsequent de-trending of the result of applying a box-car filter to the best fitting power-law was not applied to the model data because no large scale dust distribution (such as a modified fan model) was included. The synthetic map was then compared to a real map over  $45.25^\circ \leq \lambda' \leq 54.75^\circ$  and the full mapped range of ecliptic latitudes: this corresponds to 340 data points. The variance associated with each data point was taken to be constant for each data map and estimated by calculating the mean variance from a constant mean value across all cells with  $\lambda' = 44.25^\circ, 44.75^\circ, 55.25^\circ$  and  $55.75^\circ$ . In addition to the model parameters described in the main paper, a further variable in the fitting process was an offset surface brightness value ( $\alpha_0$ ), to allow for the de-trending process not resulting in variation around zero in regions of the surface brightness maps which are used for model fitting. Hence there are five free parameters in the fitting process,  $n_{0,\theta}$ ,  $n_{1,\theta}$ ,  $r_0$ ,  $r_1$ , and  $\alpha_0$ , and consequently 335 degrees of freedom.

## **Supplementary Text**

### Author notes

MHJ led the project and developed the analysis and modeling software. DB and DSB provided expertise on the HI-2 data including specific details on the pointing and photometry of the instrument, they also provided test data and contributed to the analysis. All authors contributed to the writing of the paper.

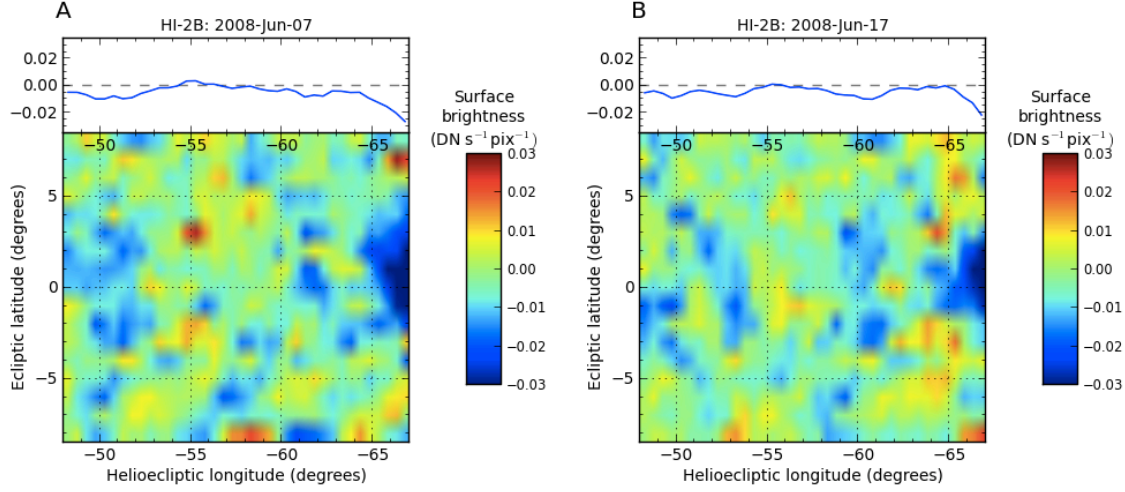


**Fig. S1.**

Surface brightness maps (lower panel) and mean scans (upper panel) for a region away from the orbit of Venus. These maps are offset by  $10^\circ$  in heliocentric longitude away from the Sun from the map shown in Figure 2A, and hence do not view the orbit of Venus. Both maps correspond to 10-day integrations of HI-2B data, and units are as in Figure 2A. **(A)** For the data set starting on 2009-Jun-7 00:00 UTC (as in Figure 2A). **(B)** For the next data set in the sequence, i.e. starting on 2009-Jun-17 00:00 UTC.

Comparison of these two maps shows that the pattern of small scale fluctuations is similar between the two, except that the features shift by about  $-10^\circ$  in heliocentric longitude between A and B (e.g. features near  $(\lambda', \beta)$   $(-55^\circ, +3^\circ)$  in A and  $(-64^\circ, +3^\circ)$  in B). This is consistent with the motion of the celestial sphere, suggesting that distant astronomical background is a component of the residual signal in these maps. The dark blue region on the right hand edge of both maps arises from a systematic error in the de-trending process due to the presence of the Earth in the instrument field-of-view at  $\lambda' \approx -70^\circ$ .

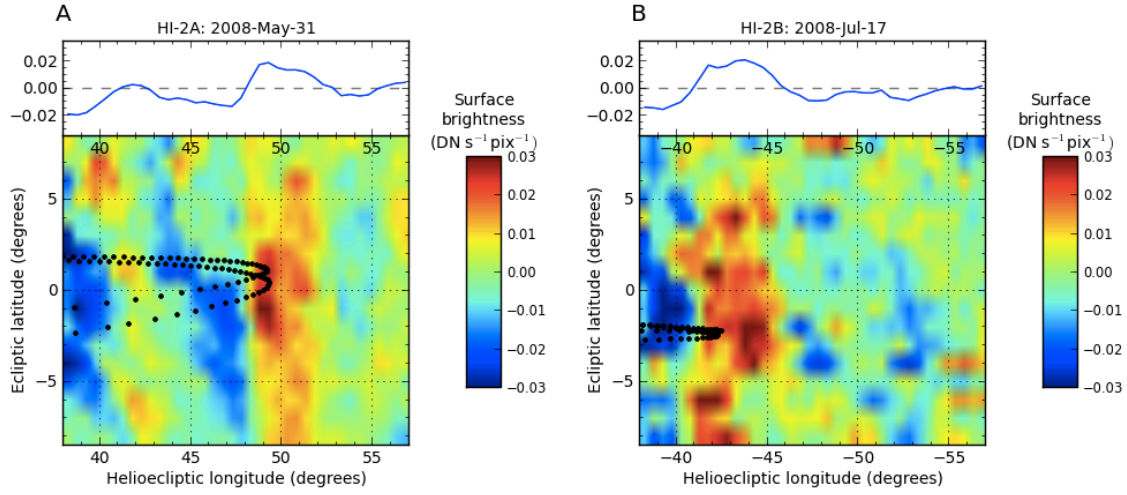


**Fig. S2**

Surface brightness maps (lower panel) and mean scans (upper panel) for two data sets at which the tangent point have similar azimuthal angles with respect to Venus ( $\theta=170^\circ$ ), but viewed from different spacecraft. Both maps correspond to 10-day integrations and units are as in Figure 2A. The orbit of Venus as viewed from the spacecraft at the start and end of the integration time is shown by black dots. **(A)** For the HI-2A data set starting on 2008-May-31 00:00 UTC. **(B)** For the HI-2B data set starting on 2008-Jul-17 00:00 UTC.

**Table S1.**

Best-fitting parameter values and 1- $\sigma$  uncertainties corresponding to the data and models presented in Figure 3.

| Data set    | $\chi^2_\nu$ | $a_0$<br>(DN s <sup>-1</sup> pix <sup>-1</sup> ) | $\frac{n_{0,\theta}}{n_{\text{fan},\nu}}$ | $\frac{n_{\text{L},\theta}}{n_{\text{fan},\nu}}$ | $r_0$<br>(AU)       | $r_1$<br>(AU)       |
|-------------|--------------|--|---|--|---------------------|---------------------|
| 2009-Jun-09 | 0.998        | -0.0010<br>±0.0003                               | 0.076±0.003                               | 0.095±0.004                                      | 0.71490<br>±0.00007 | 0.73958<br>±0.00045 |
| 2009-Jun-29 | 1.408        | -0.0014<br>±0.0003                               | 0.068±0.003                               | 0.106±0.004                                      | 0.71543<br>±0.00013 | 0.74001<br>±0.00039 |
| 2009-Jul-19 | 1.489        | -0.0031<br>±0.0003                               | 0.052±0.003                               | 0.092±0.004                                      | 0.71383<br>±0.00032 | 0.74076<br>±0.00056 |
| 2008-Nov-12 | 1.174        | 0.0007<br>±0.0003                                | 0.029±0.002                               | 0.074±0.004                                      | 0.71151<br>±0.00044 | 0.73967<br>±0.00062 |

## References and Notes

1. S. F. Dermott, S. Jayaraman, Y. L. Xu, B. Å. S. Gustafson, J. C. Liou, A circumsolar ring of asteroidal dust in resonant lock with the Earth. *Nature* **369**, 719–723 (1994). [doi:10.1038/369719a0](https://doi.org/10.1038/369719a0)
2. W. T. Reach, B. A. Franz, J. L. Weiland, M. G. Hauser, T. N. Kelsall, E. L. Wright, G. Rawley, S. W. Stemwedel, W. J. Spiesman, Observational confirmation of a circumsolar dust ring by the COBE satellite. *Nature* **374**, 521–523 (1995). [doi:10.1038/374521a0](https://doi.org/10.1038/374521a0)
3. J. M. Hahn, H. A. Zook, B. Cooper, B. Sunkara, Clementine observations of the zodiacal light and the dust content of the inner solar system. *Icarus* **158**, 360–378 (2002). [doi:10.1006/icar.2002.6881](https://doi.org/10.1006/icar.2002.6881)
4. D. Nesvorný, P. Jenniskens, H. F. Levison, W. F. Bottke, D. Vokrouhlický, M. Gounelle, Cometary origin of the zodiacal cloud and carbonaceous micrometeorites. Implications for hot debris disks. *Astrophys. J.* **713**, 816–836 (2010). [doi:10.1088/0004-637X/713/2/816](https://doi.org/10.1088/0004-637X/713/2/816)
5. M. Rowan-Robinson, B. May, An improved model for the infrared emission from the zodiacal dust cloud: cometary, asteroidal and interstellar dust. *Mon. Not. R. Astron. Soc.* **429**, 2894–2902 (2013). [doi:10.1093/mnras/sts471](https://doi.org/10.1093/mnras/sts471)
6. J. A. Burns, P. L. Lamy, S. Soter, Radiation forces on small particles in the solar system. *Icarus* **40**, 1–48 (1979). [doi:10.1016/0019-1035\(79\)90050-2](https://doi.org/10.1016/0019-1035(79)90050-2)
7. A. A. Jackson, H. A. Zook, A solar system dust ring with the Earth as its shepherd. *Nature* **337**, 629–631 (1989). [doi:10.1038/337629a0](https://doi.org/10.1038/337629a0)
8. S. J. Weidenschilling, A. A. Jackson, Orbital resonances and Poynting-Robertson drag. *Icarus* **104**, 244–254 (1993). [doi:10.1006/icar.1993.1099](https://doi.org/10.1006/icar.1993.1099)
9. A. J. Mustill, M. C. Wyatt, A general model of resonance capture in planetary systems: first- and second-order resonances. *Mon. Not. R. Astron. Soc.* **413**, 554–572 (2011). [doi:10.1111/j.1365-2966.2011.18201.x](https://doi.org/10.1111/j.1365-2966.2011.18201.x)
10. M. J. Kuchner, W. T. Reach, M. E. Brown, A search for resonant structures in the zodiacal cloud with COBE DIRBE: The Mars wake and Jupiter's Trojan clouds. *Icarus* **145**, 44–52 (2000). [doi:10.1006/icar.1999.6318](https://doi.org/10.1006/icar.1999.6318)
11. V. A. Krasnopolsky, A. A. Krysko, Venera 9, 10 - Is there a dust ring around Venus? *Planet. Space Sci.* **27**, 951–957 (1979). [doi:10.1016/0032-0633\(79\)90025-4](https://doi.org/10.1016/0032-0633(79)90025-4)
12. C. Leinert, B. Moster, Evidence for dust accumulation just outside the orbit of Venus. *Astron. Astrophys.* **472**, 335–340 (2007). [doi:10.1051/0004-6361:20077682](https://doi.org/10.1051/0004-6361:20077682)
13. M. J. Kuchner, M. J. Holman, The geometry of resonant signatures in debris disks with planets. *Astrophys. J.* **588**, 1110–1120 (2003). [doi:10.1086/374213](https://doi.org/10.1086/374213)
14. C. C. Stark, M. J. Kuchner, The detectability of exo-Earths and super-Earths via resonant signatures in exozodiacal clouds. *Astrophys. J.* **686**, 637–648 (2008). [doi:10.1086/591442](https://doi.org/10.1086/591442)

15. P. Kalas, J. R. Graham, M. Clampin, A planetary system as the origin of structure in Fomalhaut's dust belt. *Nature* **435**, 1067–1070 (2005). [Medline](#)  
[doi:10.1038/nature03601](https://doi.org/10.1038/nature03601)
16. M. L. Kaiser, T. A. Kucera, J. M. Davila, O. C. Cyr, M. Guhathakurta, E. Christian, The STEREO mission: An introduction. *Space Sci. Rev.* **136**, 5–16 (2008).  
[doi:10.1007/s11214-007-9277-0](https://doi.org/10.1007/s11214-007-9277-0)
17. C. Eyles, R. A. Harrison, C. J. Davis, N. R. Waltham, B. M. Shaughnessy, H. C. A. Mapson-Menard, D. Bewsher, S. R. Crothers, J. A. Davies, G. M. Simnett, R. A. Howard, J. D. Moses, J. S. Newmark, D. G. Socker, J.-P. Halain, J.-M. Defise, E. Mazy, P. Rochus, The Heliospheric Imagers onboard the STEREO mission. *Sol. Phys.* **254**, 387–445 (2009). [doi:10.1007/s11207-008-9299-0](https://doi.org/10.1007/s11207-008-9299-0)
18. D. S. Brown, D. Bewsher, C. J. Eyles, Calibrating the pointing and optical parameters of the STEREO Heliospheric Imagers. *Sol. Phys.* **254**, 185–225 (2009).  
[doi:10.1007/s11207-008-9277-6](https://doi.org/10.1007/s11207-008-9277-6)
19. E. Grün, H. A. Zook, H. Fechtig, R. H. Giese, Collisional balance of the meteoritic complex. *Icarus* **62**, 244–272 (1985). [doi:10.1016/0019-1035\(85\)90121-6](https://doi.org/10.1016/0019-1035(85)90121-6)
20. S. Kouchmy, P. L. Lamy, The F-corona and the circum-solar dust evidences and properties, in *Properties and Interactions of Interplanetary Dust*, R. H. Giese, P. Lamy, Eds. (Reidel, Dordrecht, Netherlands, 1985), pp. 63–74.
21. T. Kelsall, J. L. Weiland, B. A. Franz, W. T. Reach, R. G. Arendt, E. Dwek, H. T. Freudenreich, M. G. Hauser, S. H. Moseley, N. P. Odegard, R. F. Silverberg, E. L. Wright, The COBE diffuse infrared background experiment search for the cosmic infrared background. II. Model of the interplanetary dust cloud. *Astrophys. J.* **508**, 44–73 (1998). [doi:10.1086/306380](https://doi.org/10.1086/306380)
22. Materials and methods are available as supplementary materials on *Science* Online.
23. S. S. Hong, Henyey-Greenstein representation of the mean volume scattering phase function for zodiacal dust. *Astron. Astrophys.* **146**, 67–75 (1985).
24.  $n_{\text{fan},v}$  was found using a modified fan model (21) with optical scattering (23) and scaled to match the mean surface brightness of the 9 June 2009 data.
25. The presence of Venus in the field of view precludes observations with  $|\theta| < 38^\circ$ .
26. W. T. Reach, Structure of the Earth's circumsolar dust ring. *Icarus* **209**, 848–850 (2010). [doi:10.1016/j.icarus.2010.06.034](https://doi.org/10.1016/j.icarus.2010.06.034)
27. <http://asd.gsfc.nasa.gov/Christopher.Stark/catalog.php>.